Simulation of CO_2 Decomposition in a Dielectric Barrier Discharge to Produce Ozone

Oi Hoong Chin[a,1], Rajhaletchumy Anpalagan[a], Nur Hidayah Mohamad Atan[a], Kanesh Kumar Jayapalan[a], Haw Jiunn Woo[a,1], and Teck Yong Tou[b]

[a]*Multidisciplinary Physics Research and Services Laboratory, Department of Physics, Faculty of Science, University of Malaya, 50603 Kuala Lumpur, Malaysia*
[b]*Faculty of Engineering, Multimedia University, 63100 Cyberjaya, Malaysia.*

[1]Corresponding authors: ohchin@um.edu.my; woohj@um.edu.my

(Received: 11.12.21 ; Published: 15.7.22)

Abstract. Increase in anthropogenic greenhouse gases such as carbon dioxide has contributed to global warming and climate change. One of the mitigation strategies is to decompose CO_2 into useful products, and the dielectric barrier discharge plasma can be utilized for the decomposition process. To study the CO_2 decomposition process, a zero-dimensional chemical kinetics model comprising of a reduced set of appropriate chemical equations was used to simulate the reactions. The effect of electron density weighted by the number of current filaments per period and the current pulse duration on the chemical species involved in the process was studied and the simulated ozone output was compared to experimentally measured amount of ozone which is one of the final products from the decomposition of CO_2.

Keywords: Dielectric barrier discharge, carbon dioxide decomposition, chemical kinetic model, ozone production

INTRODUCTION

Global warming is growing at an alarming rate and fueling extreme weather conditions that make headlines in recent decades. To cite a most recent occurrence: on 30th June 2021, British Columbia, Canada was hit with a historic blistering heat wave hitting a record-high temperature of 49°C that claimed more than 230 lives [1]. It is a fact that global surface temperature has been increasing and in 2020, it recorded 1.02°C above that relative to the 1951-1980 average temperatures. This increase in global surface temperature corresponds to the declining Arctic Sea ice minimum and melting of more land ice sheets causing rising sea level [2]. This warming trend is mostly due to human activity in the name of industrialization and modernization at the expense of a relentless rising level of emitted heat-trapping 'greenhouse' gases into the atmosphere. Carbon dioxide is one such gas and it has attained a count of 416 ppm in air (in June 2021) [2], an all-time high in 650,000 years. Carbon dioxide is a long-lived greenhouse gas in the atmosphere, responsible for about two-thirds of the total energy imbalance that causes warming of the Earth [3]. Hence, it is imperative that human must mitigate this problem and

reduce the level of carbon dioxide. Techniques of carbon dioxide removal are carbon dioxide capture and storage and utilization. Utilization of carbon dioxide includes conversion into value-added products such as synthetic fuels, cement production, and chemicals products [4]. Our interest lies in the production of ozone which is one of the products from the decomposition of carbon dioxide. Ozone is a strong oxidizing agent, and it can be used for sanitization, sterilization as well as surface treatment [5]. The decomposition process involves (a) firstly dissociating the carbon dioxide molecules into oxygen atoms and carbon monoxide which itself is useful for the manufacture of organic and inorganic chemical products, followed by (b) subsequent association process of the oxygen atoms and a three-body process to form oxygen molecules and ozone (O_3) respectively. These processes can be facilitated in nonthermal plasma reactors, for example, microwave plasma, gliding arc discharge, corona discharge and dielectric barrier discharge (DBD) [6].

In a previous work [7], we reported on ozone production from dissociation of CO_2 using a water cooled coaxial DBD in filamentary AC mode. DBD is not at local thermodynamic equilibrium. The DBD reactor is usually configured with a dielectric barrier between a pair of electrodes. The purpose of inserting the dielectric barrier is to limit the amount of charge and energy imparted to the current filaments or microdischarge channels, making them short-lived and distributing these microdischarges over the entire electrode surface. With electrons in the DBD attaining temperatures of 10^3-10^4 K whilst the ions and neutral particles remaining at temperatures closer to room temperature (~10^2 K), the bulk of the discharge is near to room temperature. The advantage is this non-equilibrium condition creates rich plasma chemistry enabling many chemical reactions to take place. Another advantage of DBD is that it can be generated and maintained at atmospheric pressure making it easy to configure in an economical and reliable way. This work is not mitigating the global warming and climate change problem per se, but it offers a potential method that can be further developed for the purpose.

For better understanding of the decomposition of CO_2 to produce ozone in DBD, it is necessary to simulate the chemical kinetics of the relevant chemical reactions occurring in the discharge. A model in 2D or 3D can provide detailed plasma chemistry, but it is not possible as it is excessively costly in computation time. It will suffice to use a 0D chemical kinetics model as reported by Aerts, Martens and Bogaerts [8]. Here, we present a 0D chemical kinetics model of the decomposition of CO_2 in DBD based on reduced chemistry model of Aerts, Sommers and Bogaerts [9] using DBD parameters peculiar to the system of Ref. [7]. Simulated and measured ozone output were compared in relation to their dependence on the input voltage that determines the electron density in the microdischarges.

DBD PARAMETERS

There are various DBD parameters required for setting the conditions in the simulation and they are determined in the following manner. Details of the experimental setup were described in Ref. [7].

Residence Time

Residence time, *RT*, is the average time taken by CO_2 molecules to travel from the plane of entry to the plane of exit of the active discharge region. Taking the CO_2 flow rate of 2 L/min and assuming laminar flow, *RT* is calculated from the ratio of the active discharge volume over the

gas flow rate. With reference to the cross-sectional structure of the annular gap between the inner electrode and the quartz tube as shown in Fig. 1 and given the active discharge length to be equal to the length of the outer wire mesh electrode of 120 mm, $RT = 0.163$ s. This is equivalent to the time length of the computation.

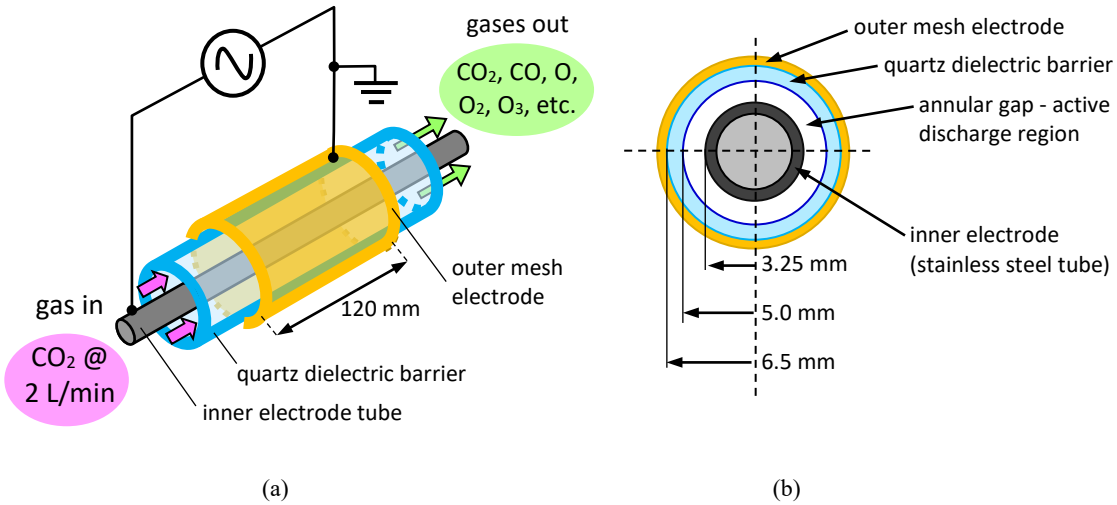

FIGURE 1. (a) Schematic arrangement and (b) cross-sectional structure of the DBD reactor.

Frequency, Plasma-On Time, Plasma-Off Time, and Rate of Microdischarge Encounter Rate

Next, we need to determine the number of microdischarges that the CO_2 molecules will encounter on their transit from the entrance plane to the exit plane of the active discharge region. From the sample set of electrical signals as shown in Fig. 2(a), the frequency, $f = 18.78$ kHz, and a half-period is 26.6 μs. It is assumed that the rate of encounter is not more than one microdischarge per half period of the applied voltage [10]. It is observed that a group of current spikes occur at the first and third quarter of each voltage cycle. Each current spike is representative of a single microdischarge. Although each group of spikes has multiple peaks, the measured current is an integrated entity over the entire discharge length, hence, the multiple microdischarges (average of 56 spikes per half-period in Fig. 2(a)) are spread over the entire expanse of the active length of 120 mm. As the CO_2 molecules traverse a particular cross-sectional plane, they will not encounter all the microdischarges within that half period. For the duration of half-period, the CO_2 molecules within an infinitesimal cross-sectional plane would only have traversed ~0.02 mm, which is 10% of the typical diameter of a microdischarge (0.2 mm) [5]. Therefore, the possibility of encountering more than one microdischarge is highly unlikely. Expanding the current waveform and measuring the time width of the current spikes at half maximum, the average FHWM are 26±8, 27±11 and 28±12 ns respectively for peak discharge voltages of 5.85, 7.05 and 8.55 kV. These values are taken to be the plasma-on time, $t_{(on)}$, during which the chemical reactions will take place and shall be computed. The plasma-off time, $t_{(off)} = 0.5f - t_{(on)}$ (in the case of one microdischarge encounter per half-period); and during this plasma-off time, the chemical reactions involving electrons will be switched off. It is

estimated that the CO_2 molecules will encounter 6128 microdischarges during their passage through the length of the active discharge region. The number of current spikes (microdischarges equivalent) per period determined for the respective peak voltages of 5.85, 7.05 and 8.55 kV are 112, 181 and 309, and the corresponding microdischarge encounter rates (proportionately estimated) are one in three ½-periods, one in two ½-periods and one in every ½-period. This corresponds to roughly 2043, 3064 and 6128 microdischarges encounters respectively within the residence time of 0.163 s.

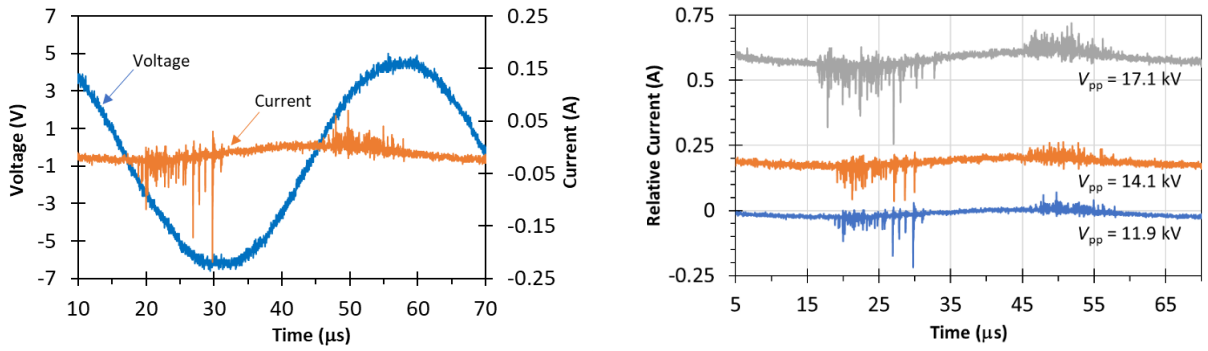

(a) (b)

FIGURE 2. (a) Sample electrical signals for V_{pp} = 11.9 kV, and (b) Current waveforms for different V_{pp}.

Electric Field, E, and Electron Density, n_e

The electric field, E, within the gap in the electrode arrangement is estimated from the peak voltage, V_0, and the dimension of the DBD reactor of Fig. 1(b) using Eq. (1).

$$E \cong \frac{0.92V_0}{\ln(b/a)}\frac{1}{r}\hat{r}; \quad b > r > a. \tag{1}$$

r is the radial dimension with a = 3.25 mm and b = 5.0 mm. The dielectric constants of the CO_2 gas gap and the quartz dielectric are 1.0 and 3.8 respectively. The factor 0.92 is determined from consideration of division of voltage across the two concentric dielectric layers in coaxial arrangement. Maximum electric field strength is at $r = a$, and the estimated value for the three V_{pp} values shown in Fig. 2(b) are listed in Table 1.

TABLE 1. Estimated maximum electric field, E_a, and the corresponding values of reduced electric field, E_a/N, where N is the CO_2 gas number density at 1 atm and 298 K, current density, J, and electron density, n_e, values. Unit of Townsend (Td) is equivalent to 10^{-17} V·cm^2.

V_{pp} (or V_p) in kV	E_a in kV·cm^{-1}	E_a/N in Td	J in A·m^{-2}	n_e in cm^{-3}
11.9 (5.95)	37	149	1.18×10^{6}	1.39×10^{13}
14.1 (7.05)	43	176	1.44×10^{6}	1.43×10^{13}
17.1 (8.55)	53	214	1.91×10^{6}	1.57×10^{13}

From Fig. 2(b), current spikes increase in number and in amplitude as the peak-to-peak voltage of the discharge is increased. This translates to higher current density, and hence larger electron density in the DBD. Taking the average of the amplitude of the current spikes that appear within one period, the electron densities were estimated as listed in Table 1. n_e is calculated using Eq. (2), [9]

$$n_e = \frac{J}{E\mu_e e}, \tag{2}$$

where J = current density of a microdischarge, E = electric field (see values in Table 1), μ_e = electron mobility in CO_2 gas and e = elementary charge (1.6×10^{-19} C). J is calculated from the average of the current spike amplitudes divided by the cross-sectional area of a microdischarge channel. The microdischarge channel is assumed to be a cylindrical plasma column of typical radius 0.1 mm [5] although it spreads onto a larger surface at the anchor point on the dielectric surface. μ_e =1447 $cm^2V^{-1}s^{-1}$ [11] for CO_2 at atmospheric pressure. The current densities are consistent with those reported in other DBD systems [5,12].

For the range of reduced electric field in DBD plasmas, the fraction of electron energy expended for vibrational processes is low and these processes were not included in the reduced chemistry model of Aerts et al. [9] Similar situation applies in this work, of which the reduced electric field, E_a/N, was estimated to have values between 149-214 Td; and within this range the vibrational reactions are not the dominant collisional processes in CO_2 discharge [14].

0D CHEMICAL KINETIC MODEL

Taking into account the generation and loss terms by chemical reactions, this 0D chemical kinetic model calculates the time evolution of the species densities using balance equations. As a zero-dimensional model, the transport processes are not explicitly included. However, the effect of the gas flow through the DBD reactor's active region is considered in terms of residence time. The DBD plasma reactor is assumed to be a batch reactor meaning the concentration of the species is uniformly distributed over the entire active volume. Exclusion of the vibrational reactions yields a simplified reduced chemistry model [9] that consists of only 17 reaction equations involving 5 neutral species (CO_2, CO, O, O_2 and O_3) and 4 charged species (electron, CO_2^+, O_2^- and O^-). The 17 reaction equations included in the model are numbered and listed below and the reaction pathways are shown in Fig. 3. M represents the third body in the respective reactions and it is represented by CO_2 molecule which has the highest concentration in this case. The rate coefficients for the respective reactions can be found in Ref. [9].

Reactions with electrons

Ionization :	$e + CO_2 \rightarrow CO_2^+ + 2e$	#1
Dissociation :	$e + CO_2 \rightarrow CO + O + e$	#2
	$e + O_3 \rightarrow O + O_2 + e$	#3
	$e + O_2 \rightarrow O + O + e$	#4
Dissociative attachment :	$e + CO_2 \rightarrow CO + O^-$	#5
	$e + O_2 \rightarrow O + O^-$	#6
Dissociative recombination :	$e + CO_2^+ \rightarrow CO + O$	#7
Electron attachment :	$e + O_2 + M \rightarrow O_2^- + M$	#8

Reactions with ions

Associative detachment :	$O^- + CO \rightarrow CO_2 + e$	#9
	$O^- + O_2 \rightarrow O_3 + e$	#10
Dissociative detachment :	$O^- + O_3 \rightarrow O_2 + O_2 + e$	#11
Dissociative recombination :	$O_2^- + CO_2^+ \rightarrow CO + O_2 + O$	#12

Reactions with neutrals

3-body recombination :	$O + O + M \rightarrow O_2 + M$	#13
	$O + O_2 + M \rightarrow O_3 + M$	#14
	$O + CO + M \rightarrow CO_2 + M$	#15
Dissociation :	$O + O_3 \rightarrow O_2 + O_2$	#16
	$O_3 + M \rightarrow O_2 + O + M$	#17

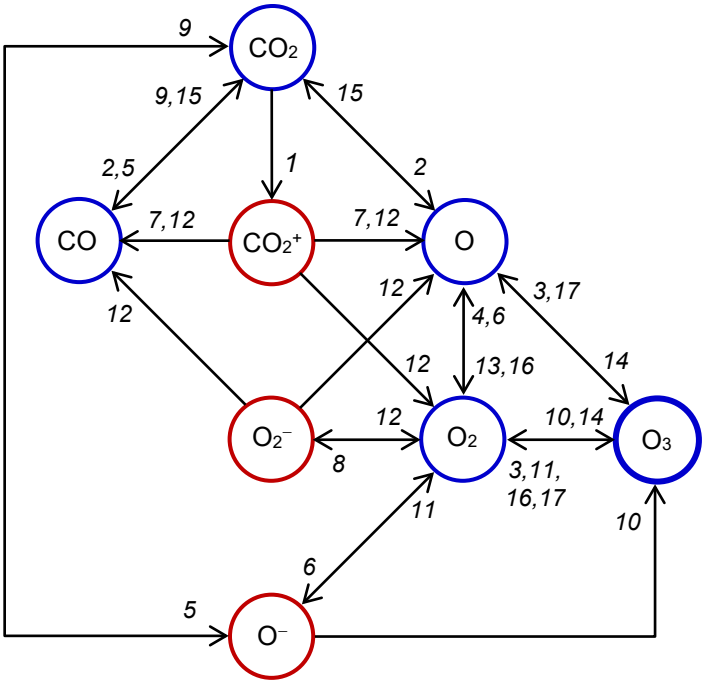

FIGURE 3. Reaction pathways of the reduced chemistry model for the simulation of CO_2 decomposition.

The time evolution of the number density of each species is computed using coupled ordinary differential equation (ODE) expressed as:

$$\frac{dn_i}{dt} = \sum_j \left[(x_{ij}^R - x_{ij}^L) k_j \prod_m n_m^L \right] \tag{3}$$

where n_i is the density of species i, x_{ij}^R and x_{ij}^L are the respective RHS and LHS stoichiometric coefficients of species i in the j-th reaction, n_m^L is the density of the m-th species in the LHS of the j-th reaction and k_j is the rate coefficient of the j-th reaction. n_i is obtained by integrating the function (3) above using MATLAB's non-stiff differential equations solver 'ode23'. The

flowchart of the computation is given in Fig. 4. The scheme of the computation is based on that of Holland's [10] used in a chemical kinetic model for reaction of methane in a DBD plasma reactor.

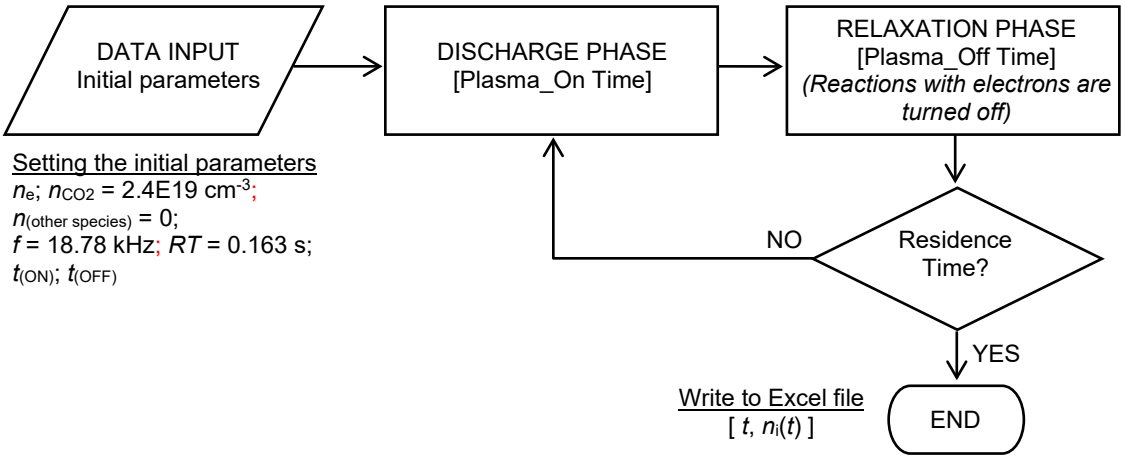

FIGURE 4. Flowchart of the computation.

RESULTS AND DISCUSSION

The computed density (averaged over each set of $t_{(on)}$ + $t_{(off)}$) for each species is plotted against time as shown in Fig. 5. It is observed that the density of CO_2 decreases gradually with time as it decomposes to other products such as CO, O, O_2, and O_3 that rises gradually. At residence time of 0.163 s, for peak discharge voltage, V_p = 5.95 kV, CO_2 decomposed by 8% and 1.25×10^{15} cm^{-3} of O_3 was produced. At higher V_p of 7.05 kV and 8.55 kV, the corresponding amount of CO_2 decomposed are 12% and 21% having generated 1.73×10^{15} cm^{-3} and 2.93×10^{15} cm^{-3} of O_3 respectively. Aerts et al. [9] had pointed out that this reduced chemical model consisted of only the most critical plasma species and reactions involved in the splitting of CO_2. A complete model would involve 42 species with 501 interacting chemical reactions that would be too computationally intensive to be handled here. The drawback is the limitation of applicability to about 15% decomposition of CO_2 as higher amount of decomposition involves more complex chemistry due to higher concentration of CO and O_2 generated. Therefore, in the case of V_p = 8.55 kV, the CO_2 decomposition calculation is applicable up to residence time of 0.105 s. Unlike Aerts et al.'s reduced chemistry model [9] of which this simulation is based on, this work did not include any dummy reactions to compensate for the consumption of electron energy contributed to the vibrational excitation of CO_2 molecules (their contribution is very minor). Another difference is the time profile of the electron density that has a slow falling long tail after the duration of the microdischarge pulse in Aerts et al.'s model [8], whereas in this work the electron density profile has been simplified into a square pulse.

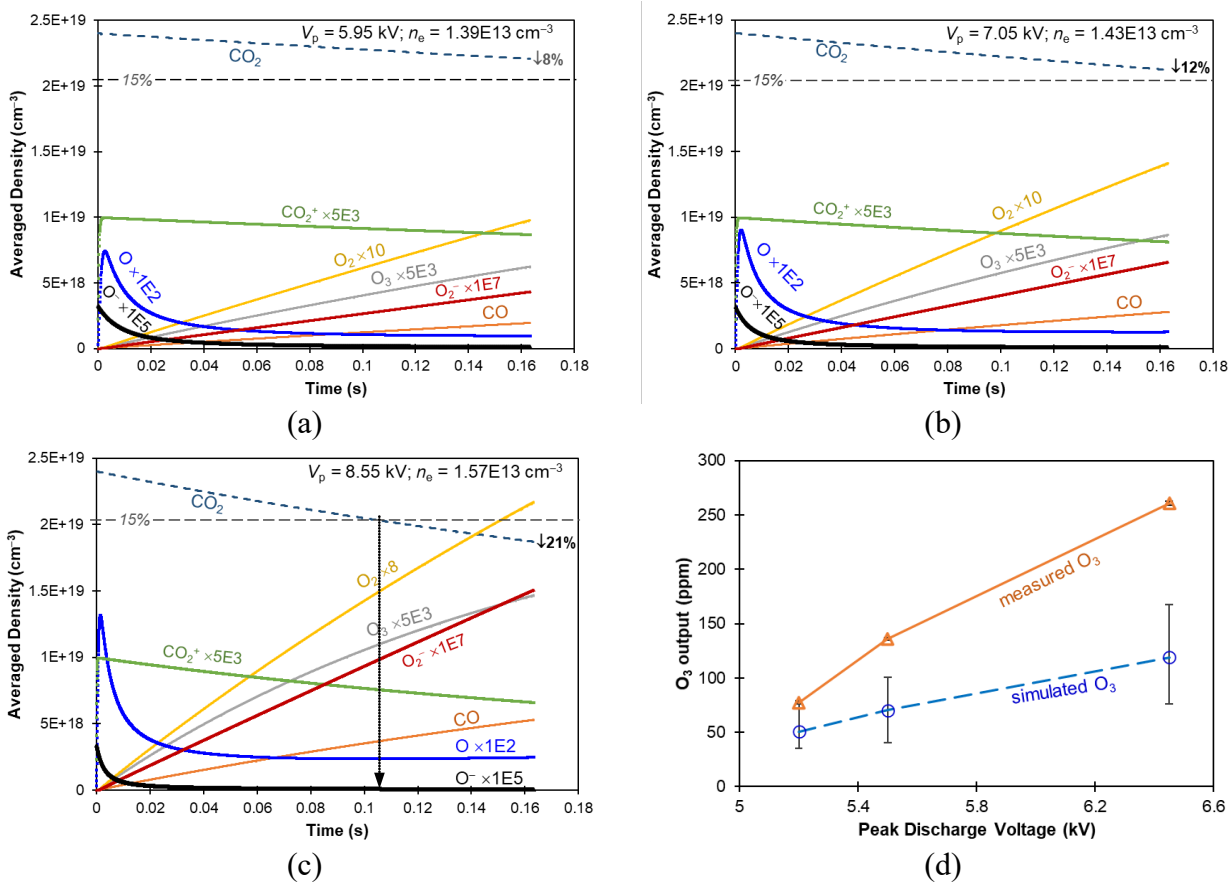

FIGURE 5. Averaged density of the various species in the reduced chemistry model for CO_2 decomposition computed for the peak discharge voltages (a) 5.95, (b) 7.05, and (c) 8.55 kV. Some of the plots are multiplied by the stated factor for visual clarity. Comparison of the measured and simulated O_3 yield is shown in (d).

When the simulated O_3 output is compared to the measured O_3 level as shown in Fig. 5(d), both the measured and simulated O_3 concentration have similar trend, rising in level as the peak discharge voltage increases. However, the magnitude in the simulated results is smaller by a factor of 0.46-0.66. Here, a conversion of O_3 number density to ppm was made by taking the O_3 concentration in air by volume to be 1 g O_3/m^3 ≡ 509 ppm O_3, given that the mass density of O_3 at 298K to be 1.963 kg/m^3 [15]. It is speculated that residual air in the DBD system would be additional sources for the splitting of the constituent oxygen molecules to form additional O_3. Furthermore, DBD plasma in atmospheric air is known to generate a considerable amount of ozone [16]. In the reduced chemistry model, the constituent oxygen molecules from residual air were not taken into consideration, hence, the amount of simulated O_3 output would be expected to be lower than the measured values. It should be mentioned that no attempt was made to determine the absolute CO_2 conversion experimentally as neither a gas chromatograph nor CO_2 gas analyzer/meter was available.

CONCLUSIONS

The simplified 0D chemical kinetic model with reduced chemistry that concentrated on the 17 most significant processes/reactions in the decomposition of CO_2 involving 5 neutral species, 3 charged ions and electrons, was able to produce similar trend of O_3 output to that obtained

experimentally when the discharge voltage was increased. However, the amount of O_3 produced at the end of the residence time of 0.163 s was approximately half of the measured level. This is probably because additional sources of oxygen containing species from residual air were not taken into consideration in the computation.

ACKNOWLEDGMENT

This work is partially supported by the University of Malaya RU Grant - Faculty Program GPF042B-2018.

REFERENCES

1. S. Moon, J. Passantino and R Riess, (June 30, 2021). More than 230 deaths reported in British Columbia amid historic heat wave, *Cable News Network*. https://edition.cnn.com/2021/06/29/americas/canada-heat-wave-deaths/index.html (Accessed on 2 July 2021).
2. H. Shaftel, S. Callery, R. Jackson, D. Bailey and S. Callery, (July 1, 2021). Global Climate Change: Vital Signs of the Planet, *NASA's Jet Propulsion Laboratory, CALTECH*. https://climate.nasa.gov/ (Accessed on 2 July, 2021).
3. R. Lindsey. (August 14, 2020). Climate Change: Atmospheric Carbon Dioxide, *National Oceanic and Atmospheric Administration (NOAA)*. https://www.climate.gov/news-features/understanding-climate/climate-change-atmospheric-carbon-dioxide (Accessed on 2 July, 2021).
4. J. Sekera and A. Lichtenberger, Assessing Carbon Capture: Public Policy, Science, and Societal Need, *Biophysical Economics and Sustainability*, **5**, 14 (2020). DOI: 10.1007/s41247-020-00080-5.
5. U. Kogelschatz, Dielectric-barrier Discharges: Their History, Discharge Physics, and Industrial Applications, *Plasma Chemistry and Plasma Processing*, **23**(1), 1-46 (2003). DOI: 10.1023/A:1022470901385.
6. A. Bogaerts and R. Snoeckx, "Plasma-Based CO_2 Conversion", in *An Economy Based on Carbon Dioxide and Water*, edited by M. Aresta et al., Switzerland AG: Springer Nature, 2019, pp. 287-325. DOI: 10.1007/978-3-030-15868-2_8.
7. V. Damideh, O.H. Chin, H.A. Gabbar, S.J. Ch'ng, and C.Y. Tan, Study of ozone concentration from CO_2 decomposition in a water cooled coaxial dielectric barrier discharge, *Vacuum*, **177**, 109370 (2020). DOI: 10.1016/j.vacuum.2020.109370.
8. R. Aerts, T. Martens, and A. Bogaerts, Influence of vibrational states on CO2 splitting by dielectric barrier discharges, *The Journal of Physical Chemistry C*, **116**, 23257-23273 (2012). DOI: 10.1021/jp307525t
9. R. Aerts, W. Somers, and A. Bogaerts, Carbon dioxide splitting in a dielectric barrier discharge plasma: a combined experimental and computational study, *ChemSusChem*, **8**(4), 702-716 (2015). DOI: 10.1002/cssc.201402818
10. G.D. Holland, "Reaction of Methane in a Dielectric Barrier Discharge Plasma Reactor", Ph.D. Thesis, Oklahoma State University, 2002.

11. Y.P. Raizer, *Gas Discharge Physics*, Berlin Heidelberg: Springer-Verlag, 1991, pp.11.
12. P. Vanraes, A. Nikiforov, A. Bogaerts, and C. Leys, Study of an AC dielectric barrier single micro-discharge filament over a water film, Scientific Report, **8**, 10919 (2018). DOI: 10.1038/s41598-018-29189-w.
13. A. Bogaerts, T. Kozak, K. Van Laer, and R. Snoeckx, Plasma-based conversion of CO_2: current status and future challenges, Faraday Discussions, **183**, 217-232 (2015). DOI: https://doi.org/10.1039/C5FD00053J.
14. B. Eliasson, W. Egli and U. Kogelschatz, Modelling of dielectric barrier discharge chemistry, *Pure & Applied Chemistry*, **66** (6), 1275-1286 (1994). DOI: 10.1351/pac199466061275.
15. Ozone Solutions, *Ozone Equations*, https://ozonesolutions.com/ozone-equations/, accessed on 28th July 2021.
16. X. Zhang, B.J. Lee, H.G. Im, and M.S. Cha, Ozone production with dielectric barrier discharge: effects of power source and humidity, IEEE Transactions on Plasma Science, 44 (10), 2288-2296 (2016). DOI: 10.1109/TPS.2016.2601246.